

# Supernova Ejecta and Dust Around Pulsar Wind Nebulae

## Collaborators:

Eli Dwek (GSFC)

Rick Arendt (GSFC)

Patrick Slane (CfA)

Steve Reynolds (NC State)

Kazik Borkowski (NC State)

John Raymond (CfA)

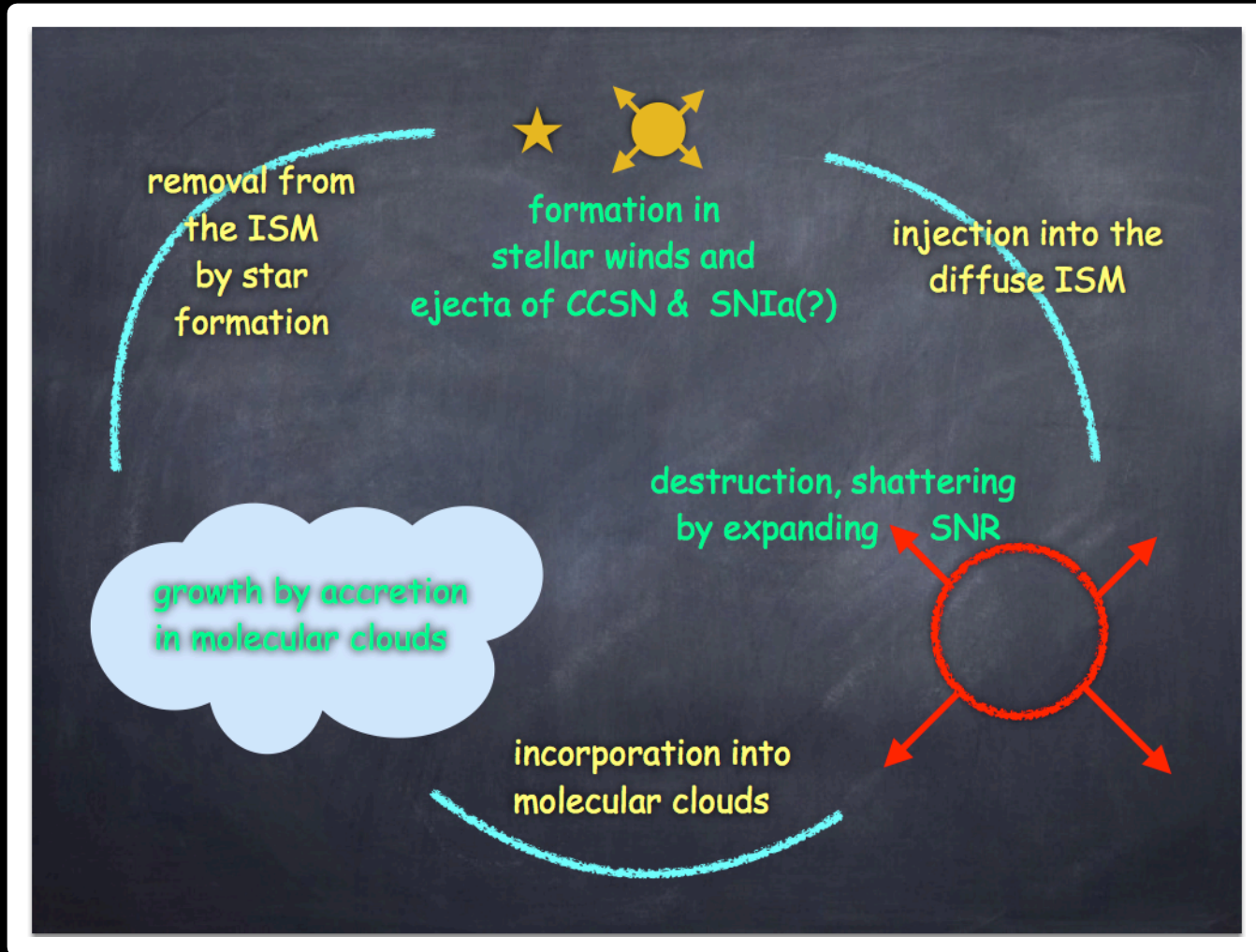
George Sonneborn (GSFC)

Yosi Gelfand (NYU Abu Dhabi)

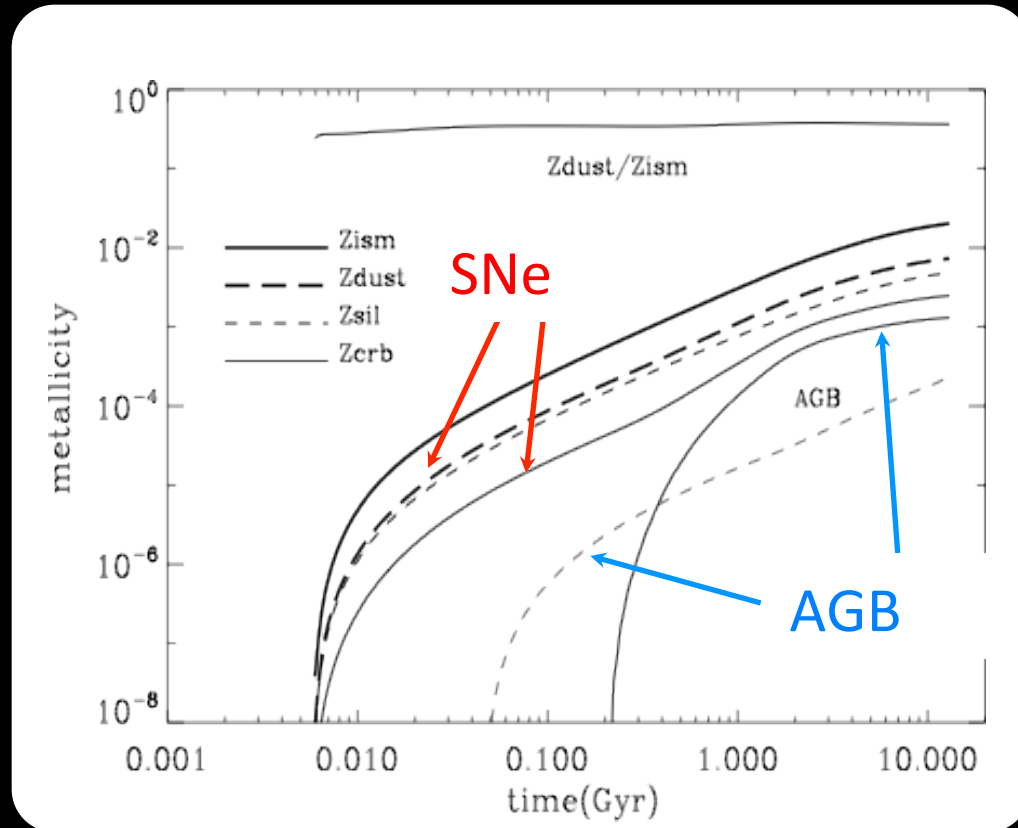
Bob Gehrz (UMN)

Tea Temim  
(STScI)

# Lifecycle of Dust



# Sources of Dust with Galactic Age



Dwek, Galliano, & Jones 2009

A young galaxy age  
< 400 Myr,  $z \geq 6$



- Intermediate mass stars have not yet reached the AGB phase
- SNe are only sources of condensed dust

An old galaxy age  
> 1 Gyr,  $z \leq 5$

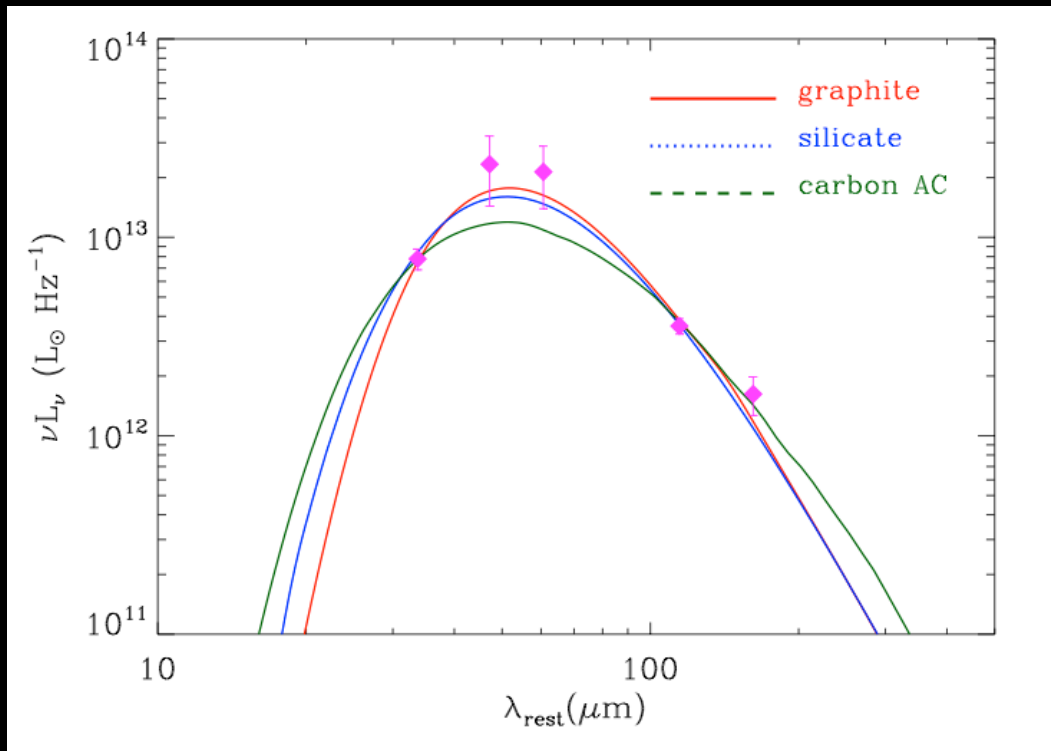


- AGB stars may be important sources of condensed dust

# Dust Masses in High-Redshift QSOs

## J1148+5251

### $z=6.4$



Dwek, Galliano & Jones 2007, ApJ, 662, 927

## Dust Masses

$3 \times 10^8 M_{\odot}$

$4 \times 10^8 M_{\odot}$

$1 \times 10^8 M_{\odot}$

$L_{\text{FIR}} \approx 2 \times 10^{13} L_{\odot}$

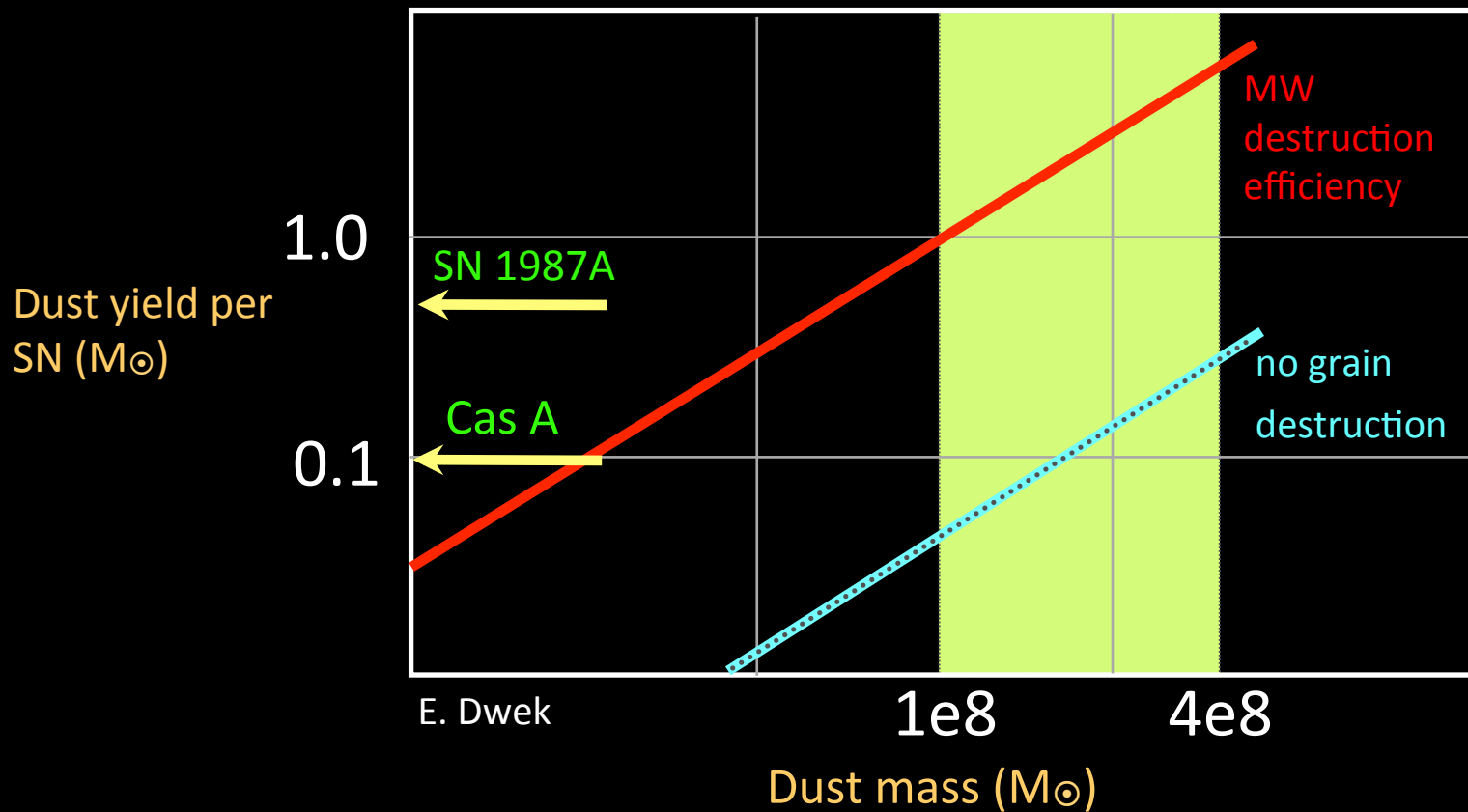
Milky Way:

$M_{\text{dust}} \approx 3 \times 10^7 M_{\odot}$

High- $z$  galaxies  $4 \leq z \leq 6.4$  show high dust masses of more than  $10^8 M_{\odot}$

# Required SN dust production rate for J1148+5251

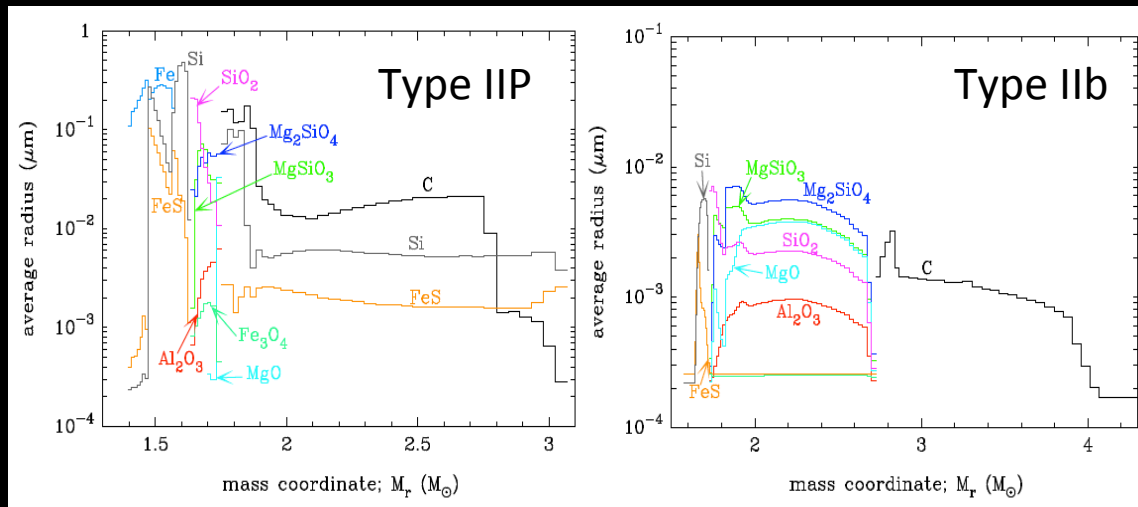
(Dwek, Galliano & Jones 2007, ApJ, 662, 927)



# Dust Formation in Supernovae: Theoretical Predictions

Models predicts SN forms  $0.1 - 1 M_{\odot}$  with  
2-20% surviving the reverse shock

Grain size and survival  
depend on SN type



Kozasa et al. 2009

Mass dominated by grains:  
>  $0.03 \mu\text{m}$  in Type IIP SNe  
<  $0.006 \mu\text{m}$  in Type IIb SNe  
(Kozasa, Nozawa et al. 2009)

# Dust Emission from Supernova Remnants

Emission originates from:

- IS/CS dust swept up by SN blast wave
- Dust condensed out of SN ejecta

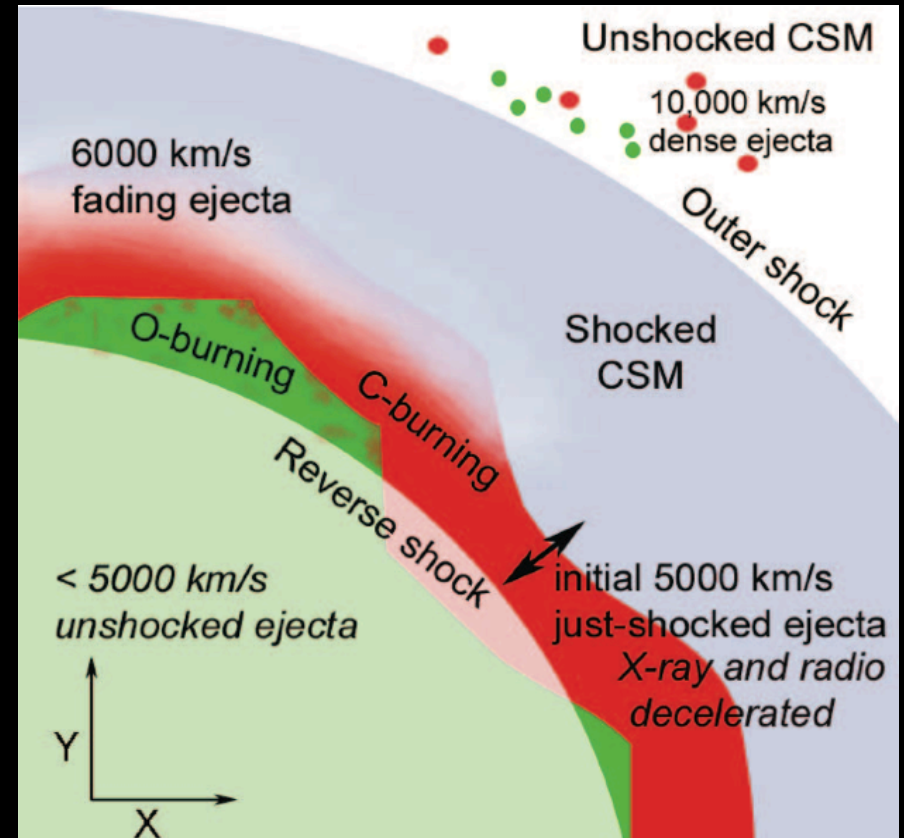
Collisionally heated dust grains:

$$\mathcal{H} = \pi a^2 n \langle v \rangle E_{dep}$$

$$\mathcal{L} = \pi a^2 \sigma T_d^4 \langle Q \rangle$$

High resolution often required to identify SN dust

## Shocked Regions in Cas A

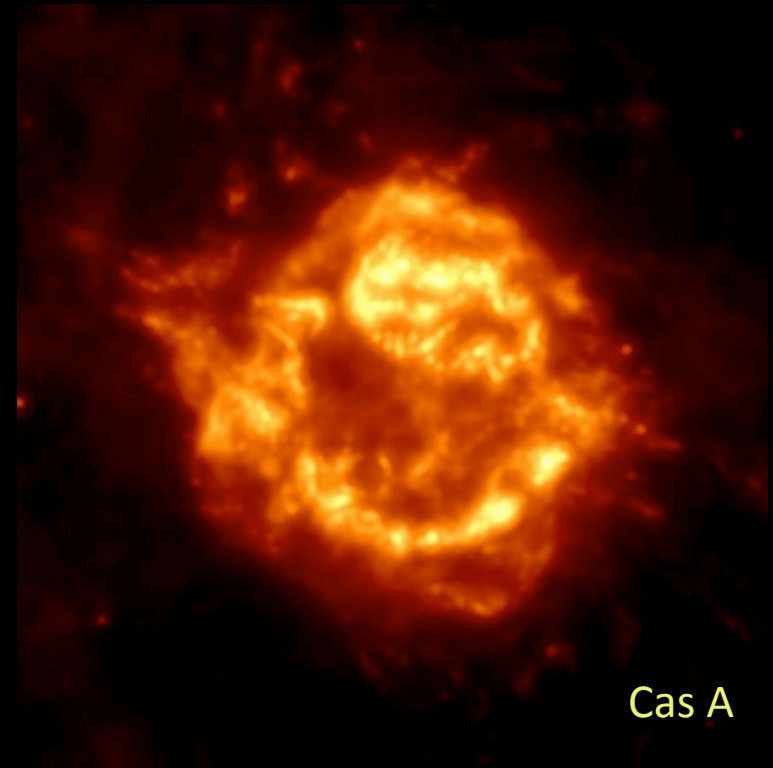


Ennis et al. 2006

# Dust Masses in SNRs

Warm SN dust confirmed in only a handful of remnants with *Spitzer* (e.g. *Rho et al. 2009*; *Ghavamian et al. 2009*, *Temim et al. 2010,2012* )

Cas A	0.02 - 0.05 $M_{\odot}$
E0102	0.007 - 0.015 $M_{\odot}$
N132D	> 0.008 $M_{\odot}$
G292.0+1.8	0.002 $M_{\odot}$



Cas A

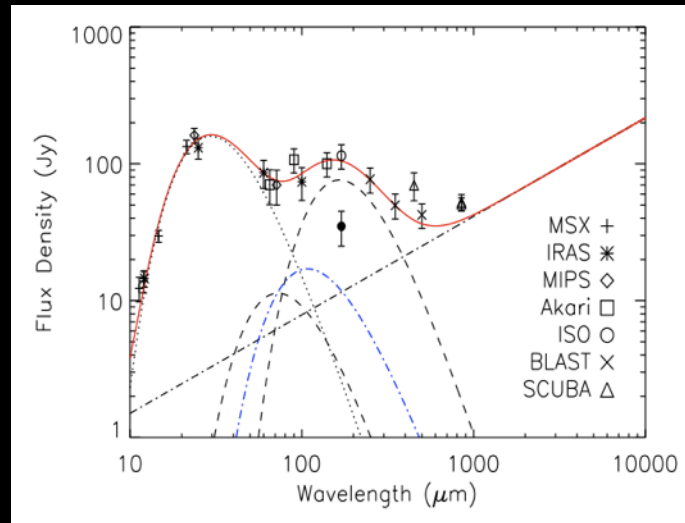
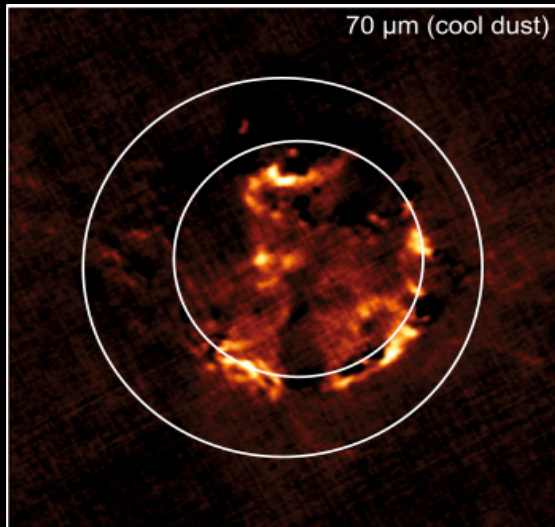
*Herschel* observations revealed cold dust!

**Cas A** > 0.1  $M_{\odot}$  (Sibthorpe et al. 2010, Barlow et al. 2010, Arendt et al. 2014, De Looze et al. 2017)

**SN 1987A** 0.5  $M_{\odot}$  (Matsuura et al. 2011, Indebetouw et al. 2013, Dwek & Arendt 2015)



# Cold dust in Cas A



Akari/Blast/Herschel  
warm ( $\sim 35$  K) dust

$\approx 0.08 M_{\odot}$

Sibthorpe et al. 2010  
Barlow et al. 2010

Dust emission spatially coincides with the X-ray emitting ejecta:  $M_d > 0.1 M_{\odot}$

(Arendt et al. 2014, De Looze et al. 2017)

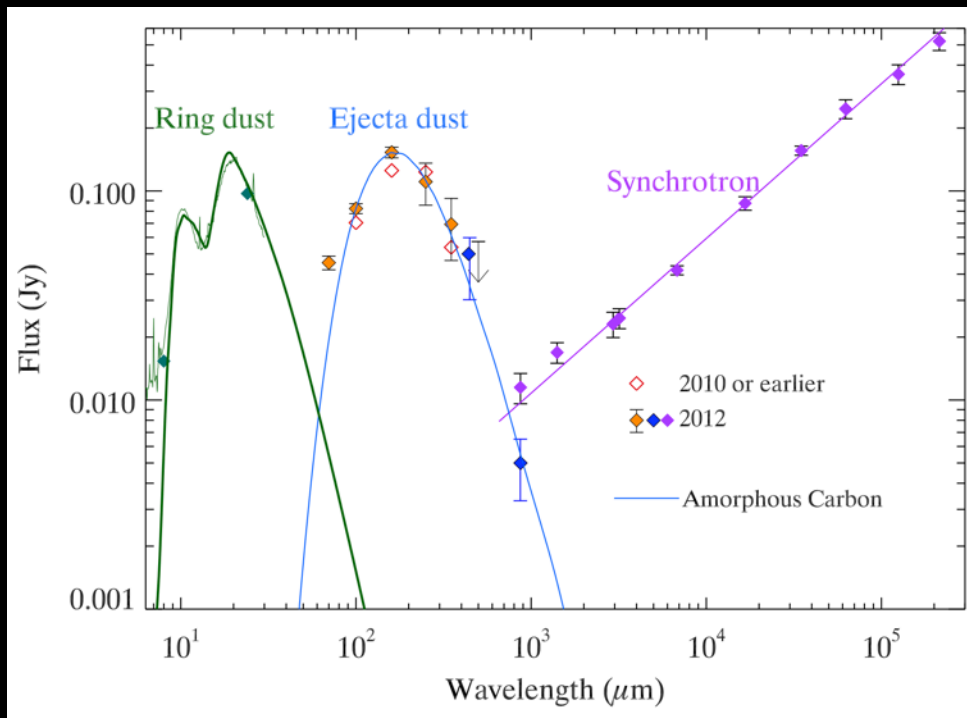
$0.8 - 1.0 M_{\odot}$  of dust formed initially and  
12-16% will survive

(Micelotta, Dwek & Slavin 2016)

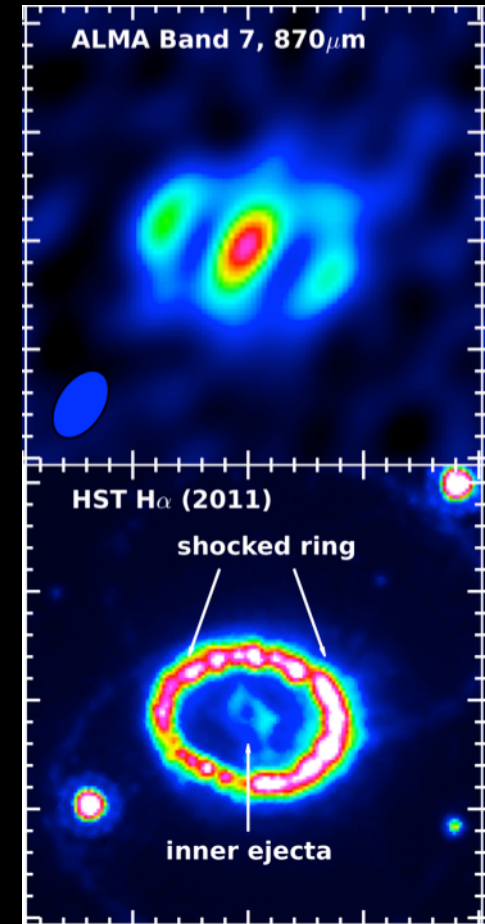
# Dust Mass in SN 1987A

Total dust mass:  $0.5 M_{\text{sun}}$

Dwek & Arendt 2015



Matsuura et al. 2011,2015

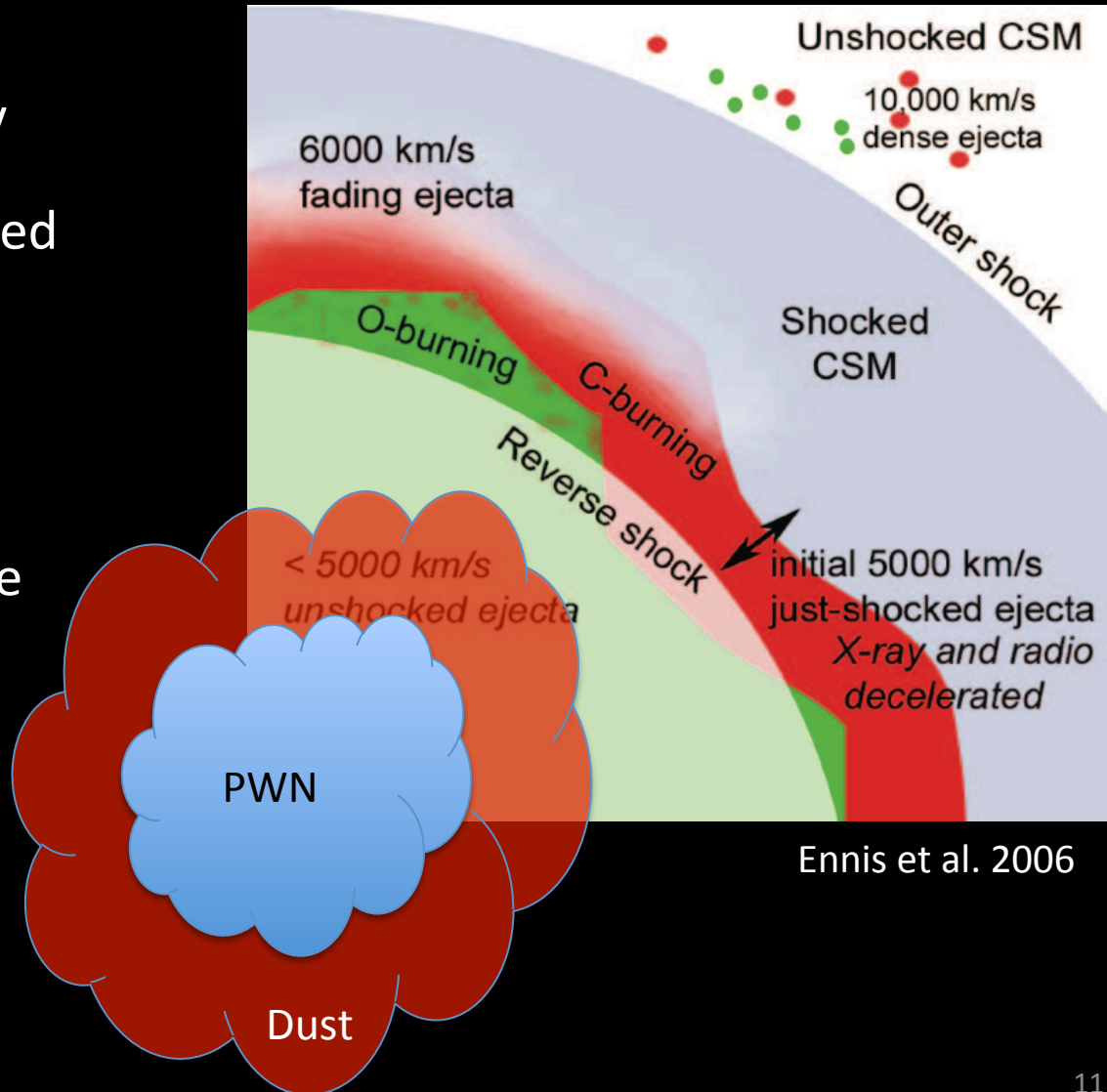


Indebetouw et al. 2013

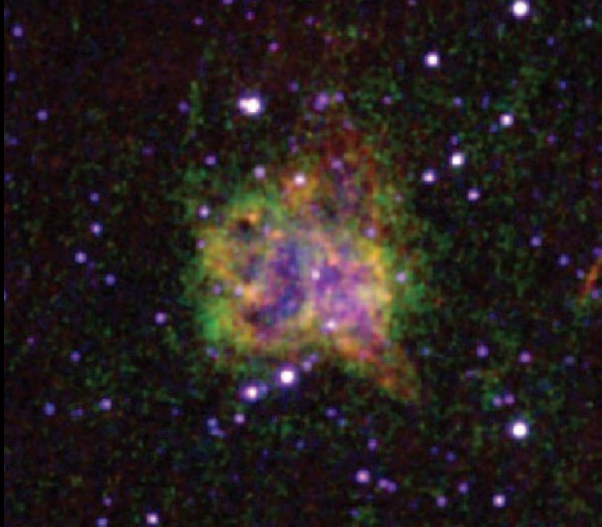
- ALMA confirms dust is associated with ejecta

# SN Ejecta & Dust Around PWNe

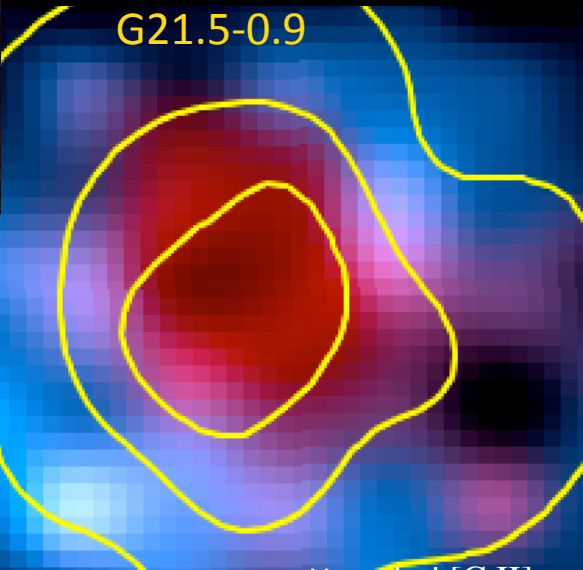
- SN dust easier to identify
- Typically radiatively heated
- Not processed by shocks
- Not mixed with ISM
- Sometimes the only place ejecta are detected



# Some Examples



B0540-69.3



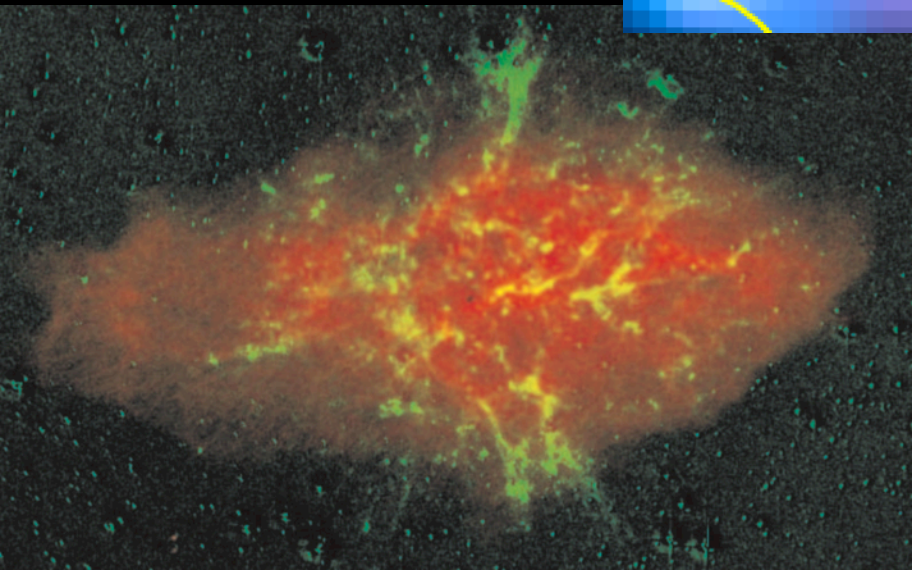
G21.5-0.9

Herschel [C II] 157  $\mu\text{m}$

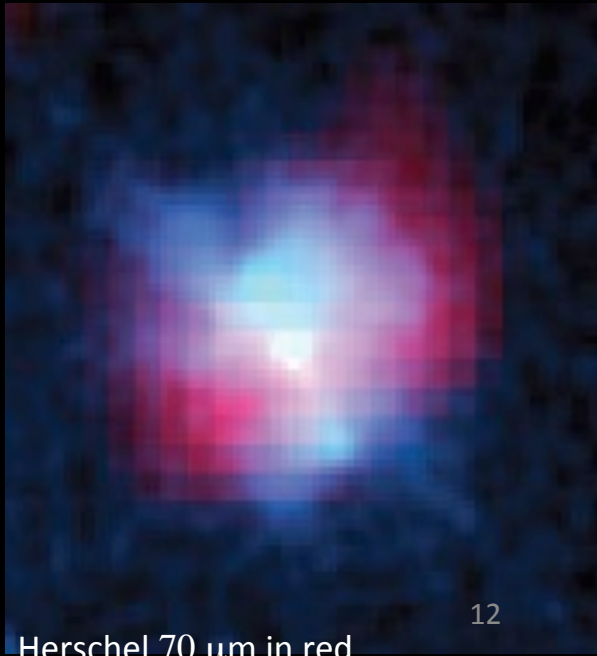


Crab Nebula

3C 58

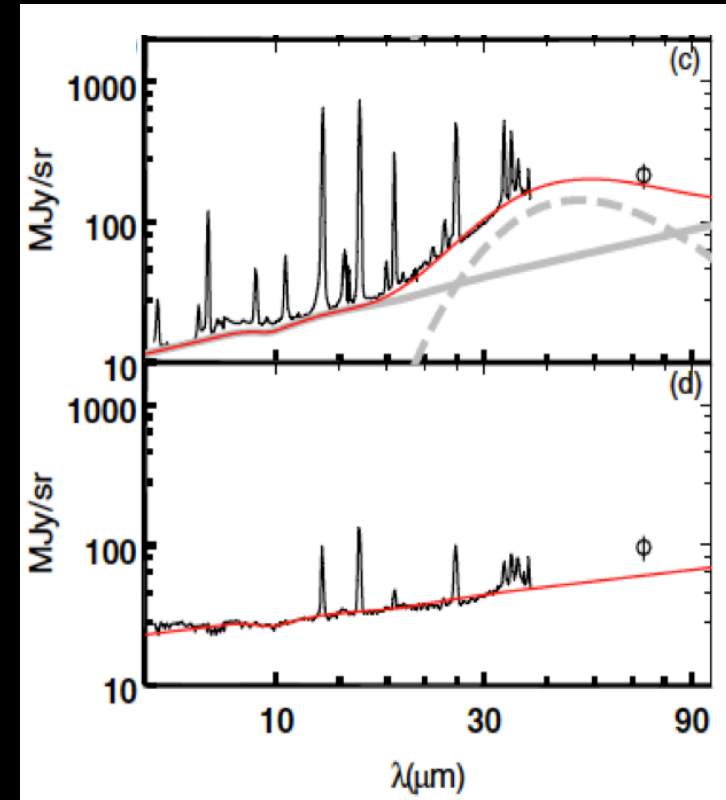
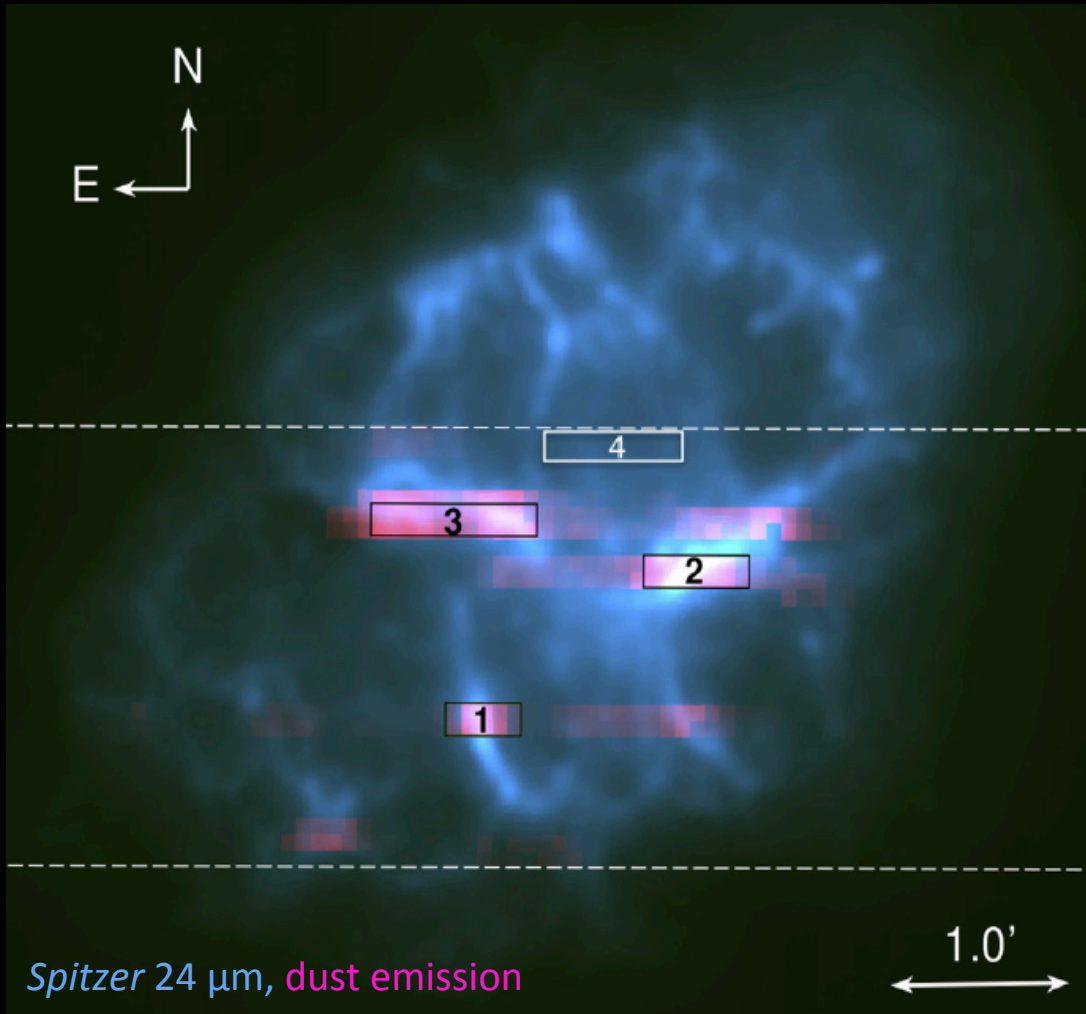


Kes 75



Herschel 70  $\mu\text{m}$  in red

# Dust in the Crab Nebula



Temim et al. 2012

Dust concentrated along the ejecta filaments

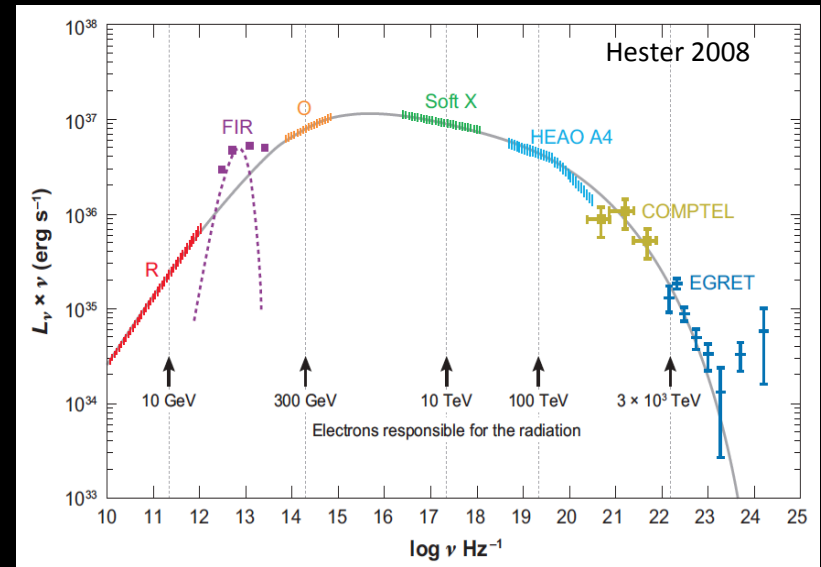
# Crab Nebula: PWN-heated Dust

Heating rate

$$H = \frac{\pi a^2 \int L_\nu Q(\nu, a) d\nu}{4\pi d^2}$$

Cooling rate

$$L = 4\pi a^2 \int \pi B_\nu(T) Q(\nu, a) d\nu$$



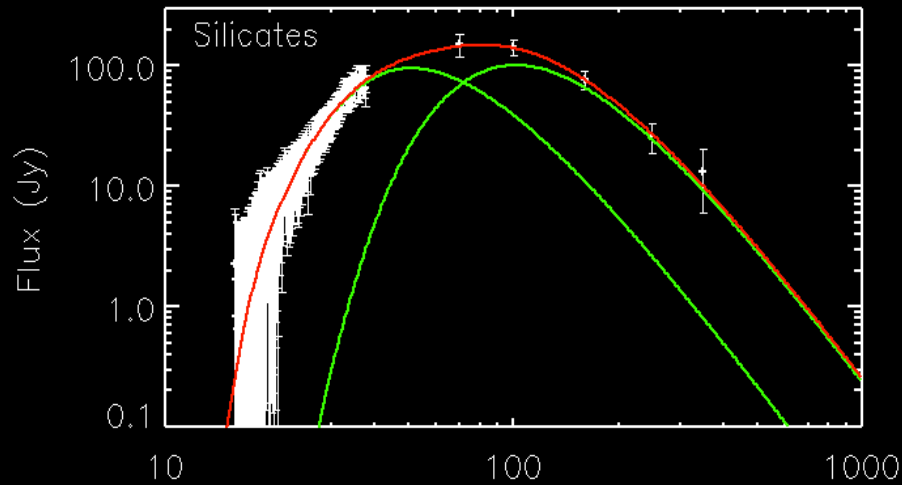
$L_\nu \rightarrow$  non-thermal spectrum of the PWN

Power-law grain size distributions of the form

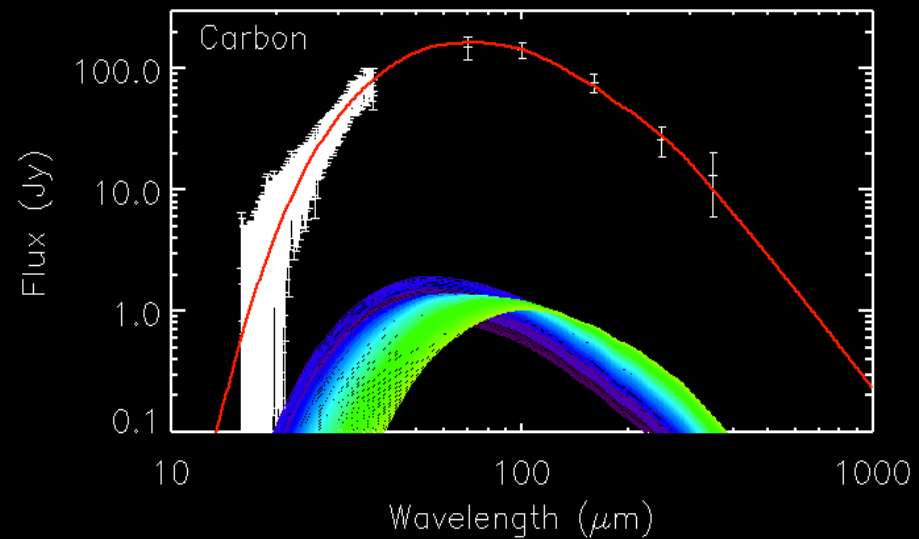
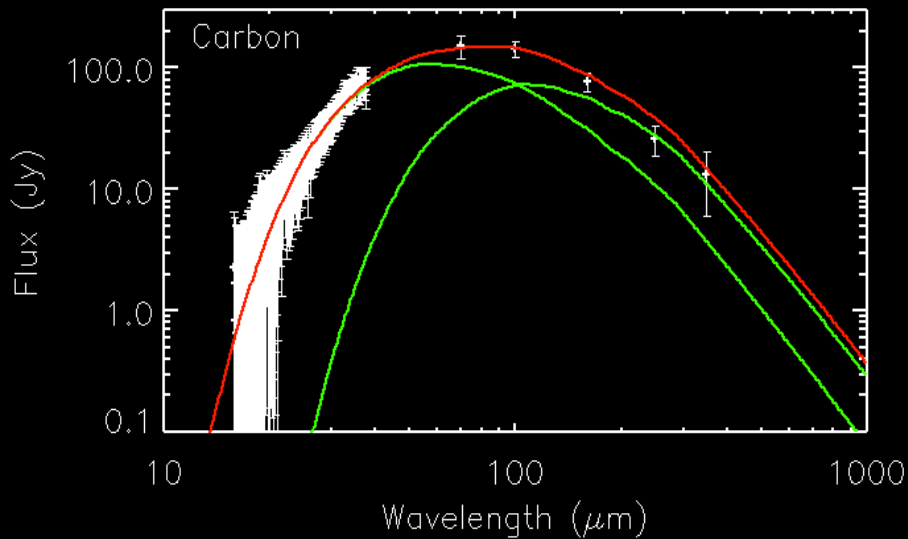
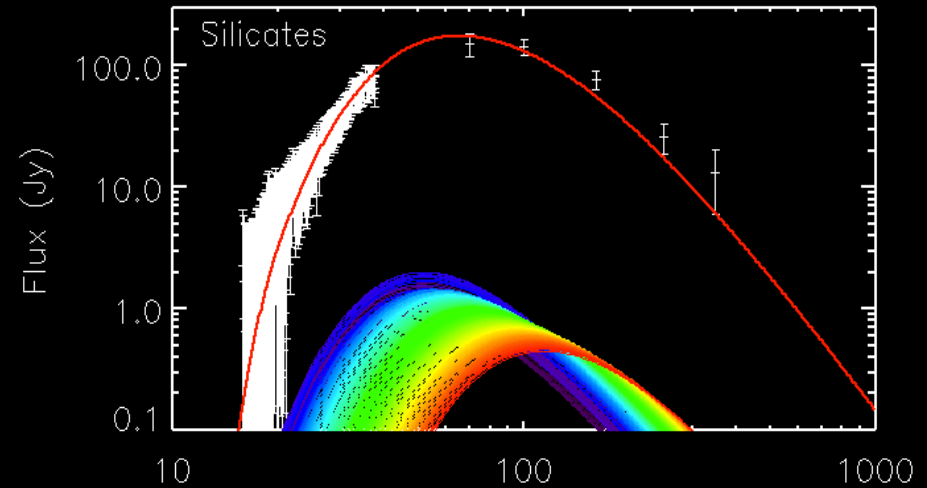
$$F(a) = a^{-\alpha}$$

Grains of different sizes heated to different temperatures  $\rightarrow$  affects the total dust mass

## Two-temperature fit



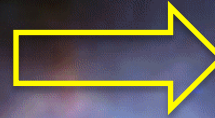
## Pulsar wind-heated model



# Revised Dust Mass in the Crab

$$M_d = 0.13 \pm 0.01 M_\odot \quad \text{silicates}$$
$$M_d = 0.02^{+0.01}_{-0.003} M_\odot \quad \text{carbon}$$

Temim & Dwek 2013



A factor of two to six less dust than previous models

Best-fit parameters:

Silicates:

$$\alpha = 3.5$$

$$a_{\max} > 0.6 \mu\text{m}$$

Carbon:

$$\alpha = 4.0$$

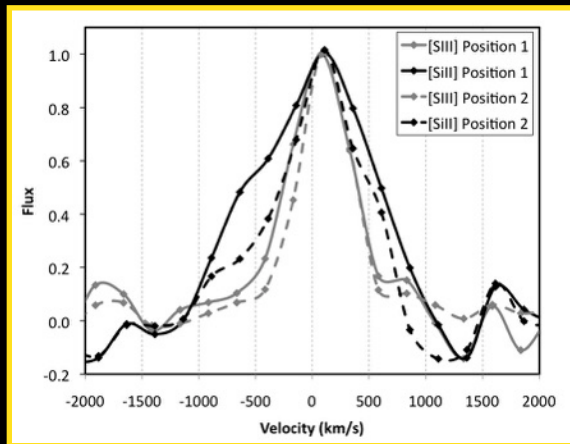
$$a_{\max} > 0.1 \mu\text{m}$$

Most of the dust mass is in the larger grains → consistent with Type IIP SN



# Dust around the PWN in G54.1+0.3

## Spitzer line emission



- Emission lines broadened to 1000 km/s
- PWN overtakes ejecta with  $v_s \sim 25$  km/s

# Dust around the PWN in G54.1+0.3

Chandra X-ray

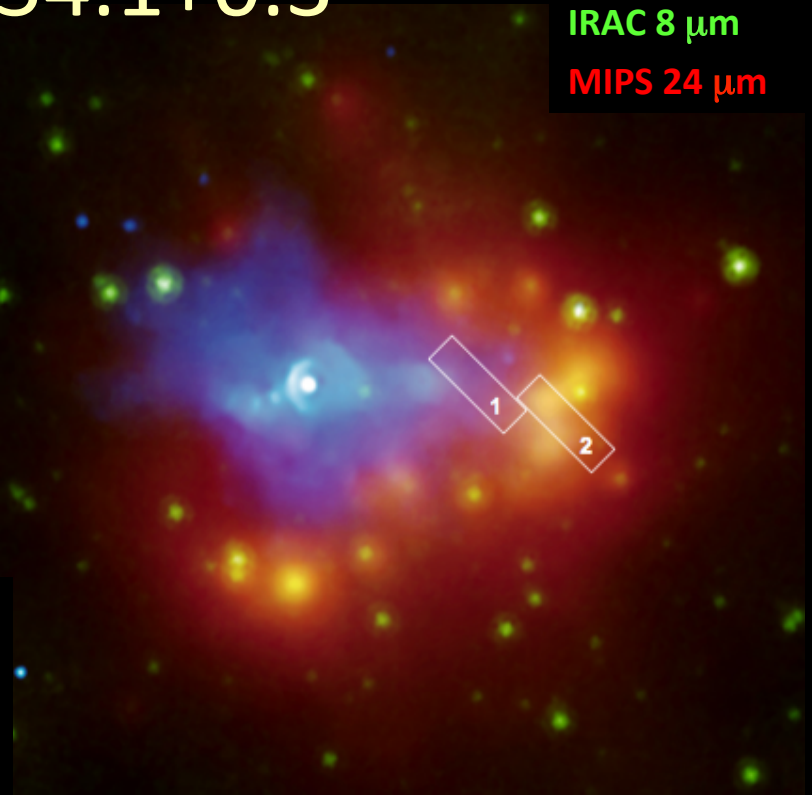
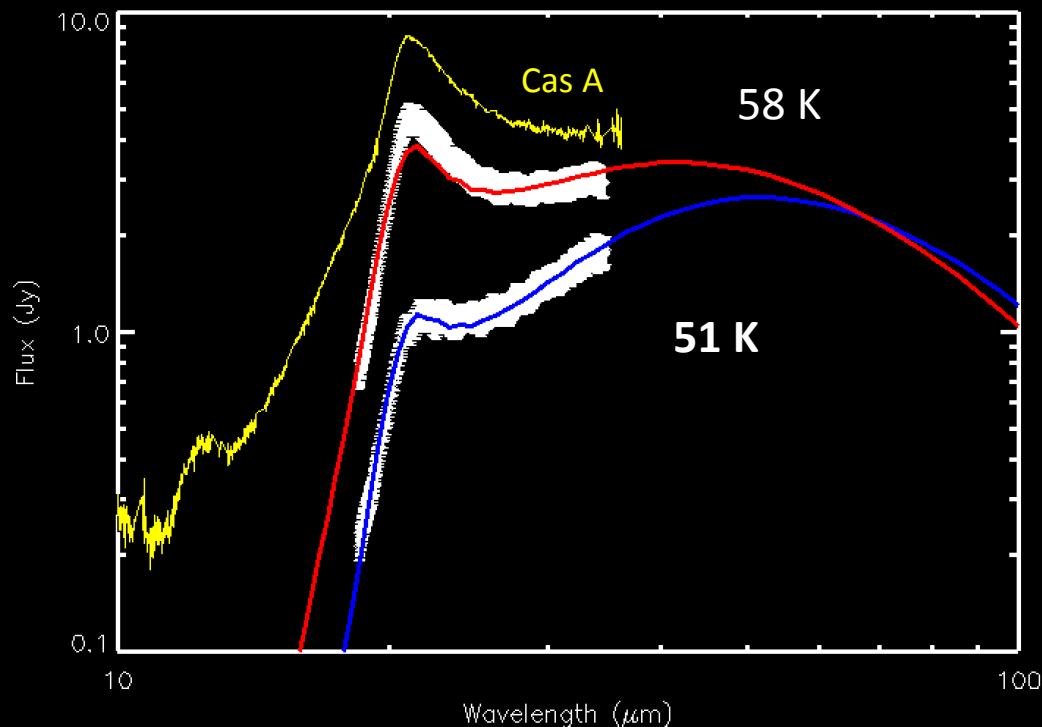
IRAC 8  $\mu\text{m}$

MIPS 24  $\mu\text{m}$

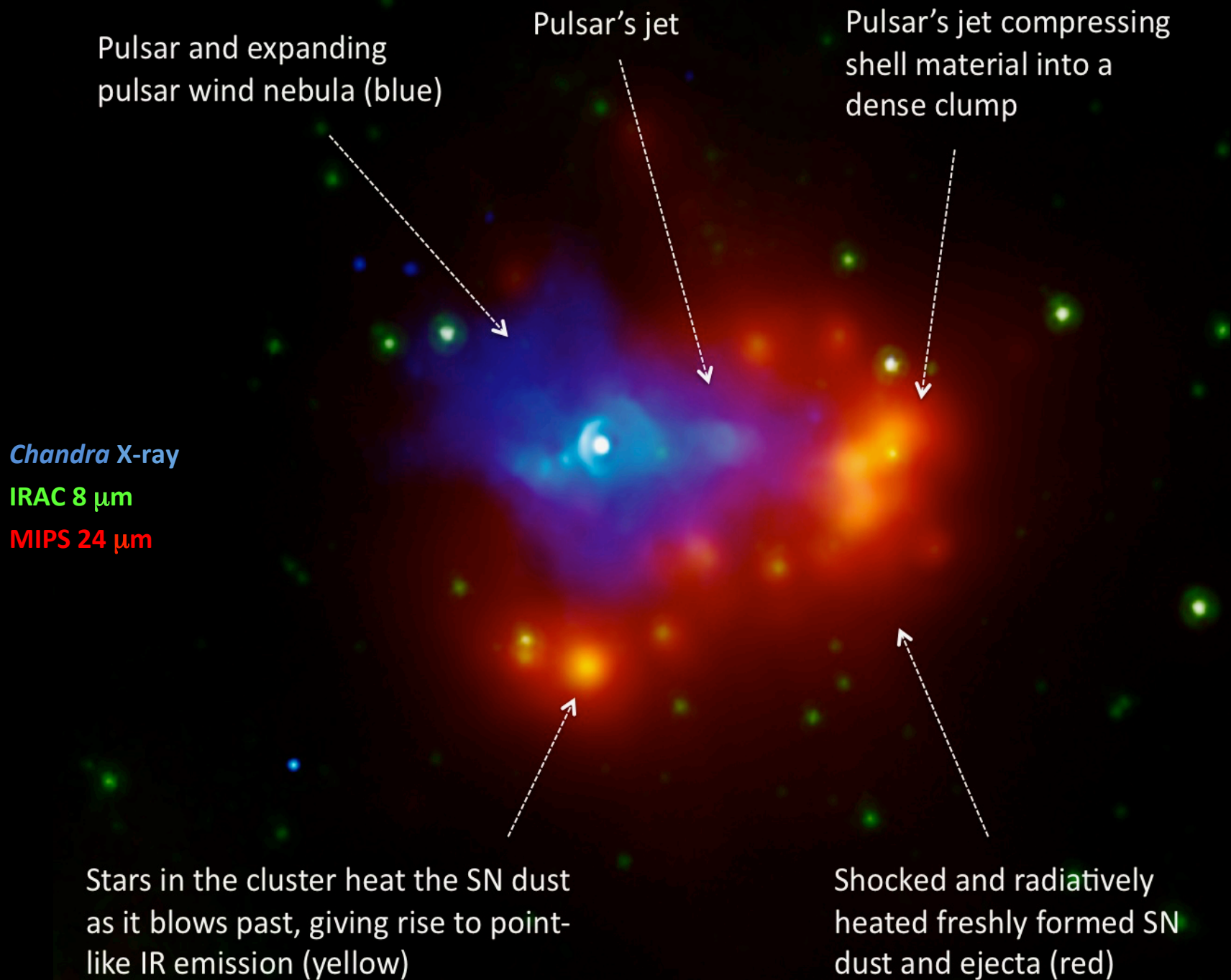
Dust composition:  $\text{Mg}_{0.7}\text{SiO}_{2.7}$   
( $\text{MgO}/\text{SiO}_2 = 0.7$ )

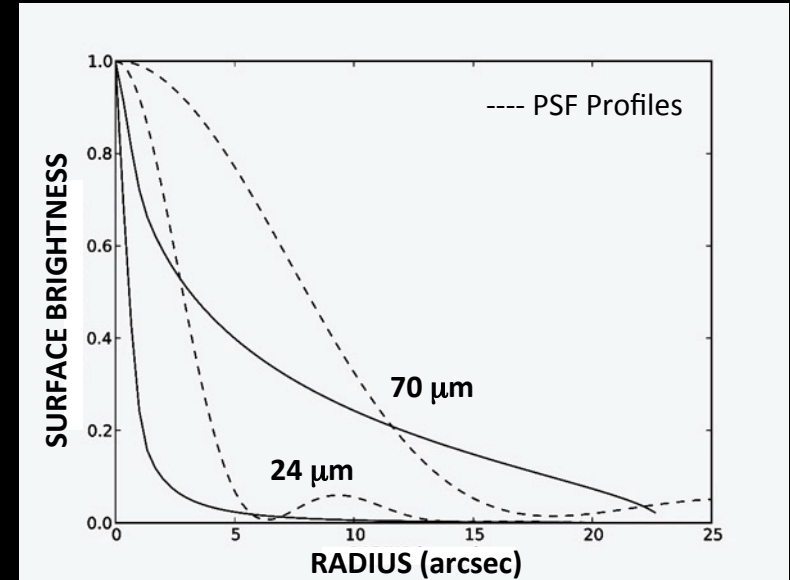
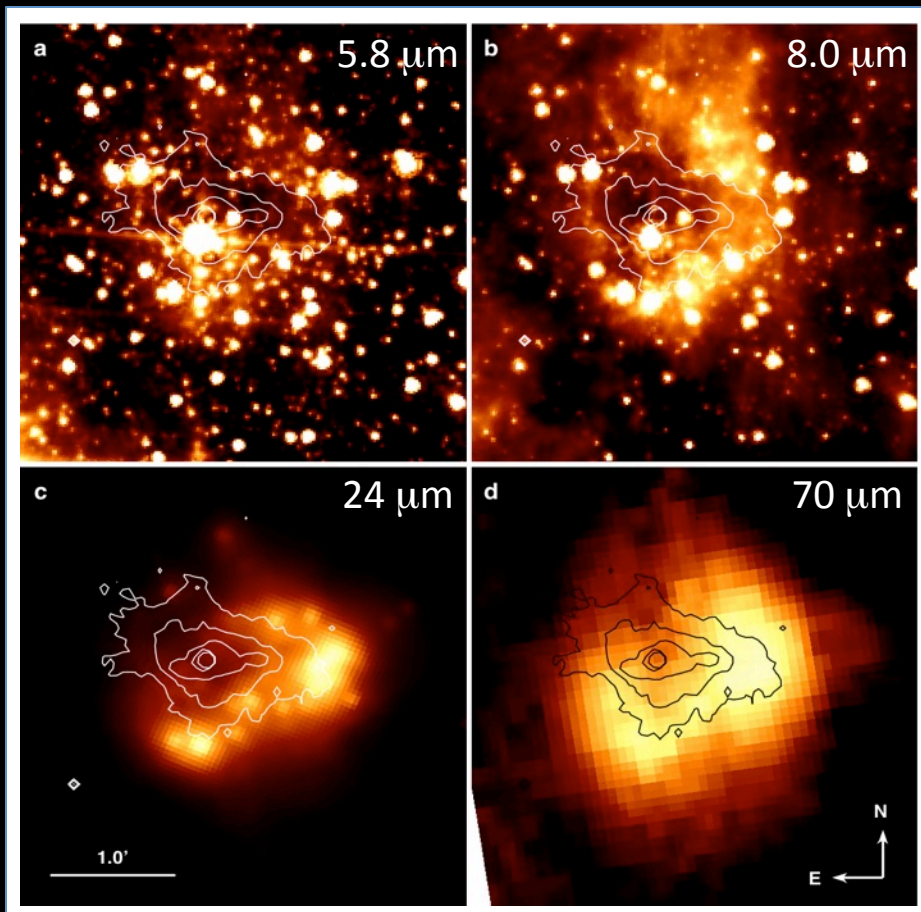
Same as in Cas A  
(Arendt et al. 2014)

Spitzer IRS spectrum



Differences in spectral shapes  
likely due to temperature  
variations





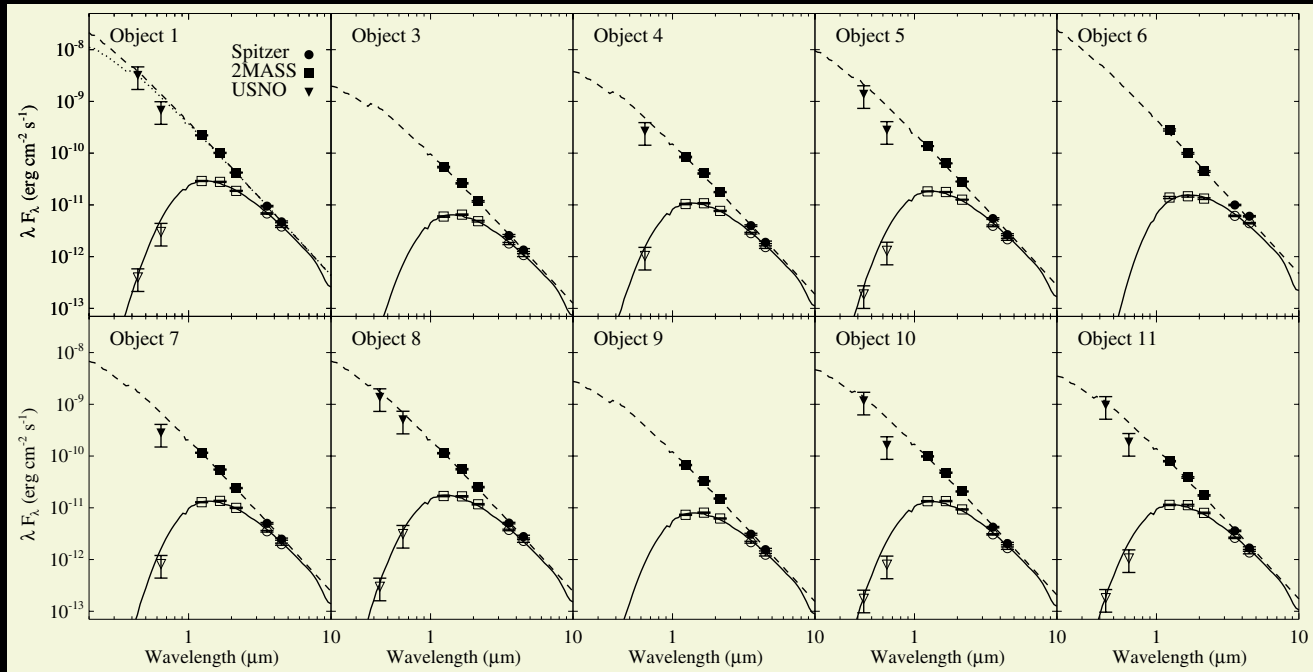
- Power law distribution of grain sizes, and a grain mass density of  $0.007 M_{\odot}/\text{pc}^3$ , heated by a main sequence B0 star with  $T=30,000 \text{ K}$
- Model shows that ejecta dust heated by main sequence stars can produce IR emission resembling point sources at 24  $\mu\text{m}$

# Kim et al. 2013: Stars in G54.1+0.3 shell are late O- to early B-type stars

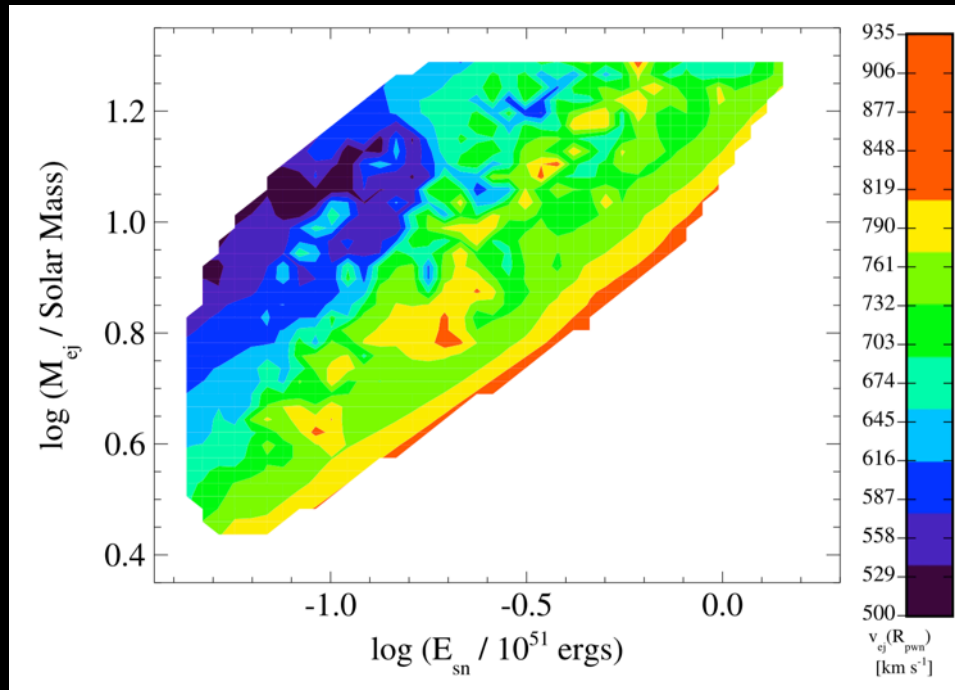
**Table 4**  
Spectral Types and Extinctions Derived in the SED Fits Using Photometric Observations with Fixed Distance of 6 kpc

Object	Temperature <sup>a,b</sup> (K)	Spectral Type	$A_V$ (mag)	$\chi^2_{\text{red}}$
1	32000	O9.5	$7.4 \pm 0.1$	2.7
2	...	...	...	...
3	20000	B2.5	$8.0 \pm 0.2$	2.3
4	23000	B1.5	$7.6 \pm 0.2$	3.0
5	27000	B0.5	$7.4 \pm 0.1$	13.0
6	33000	O9	$11.0 \pm 0.2$	11.0
7	25000	B1	$8.0 \pm 0.1$	6.8
8	26000	B1	$7.0 \pm 0.2$	4.0
9	21000	B2	$8.1 \pm 0.2$	6.6
10	24000	B1.5	$7.3 \pm 0.1$	12.2
11	22000	B2	$7.1 \pm 0.1$	6.0

Progenitor mass:  
**18-35  $M_{\odot}$**



# G54.1+0.3: Expanding Ejecta

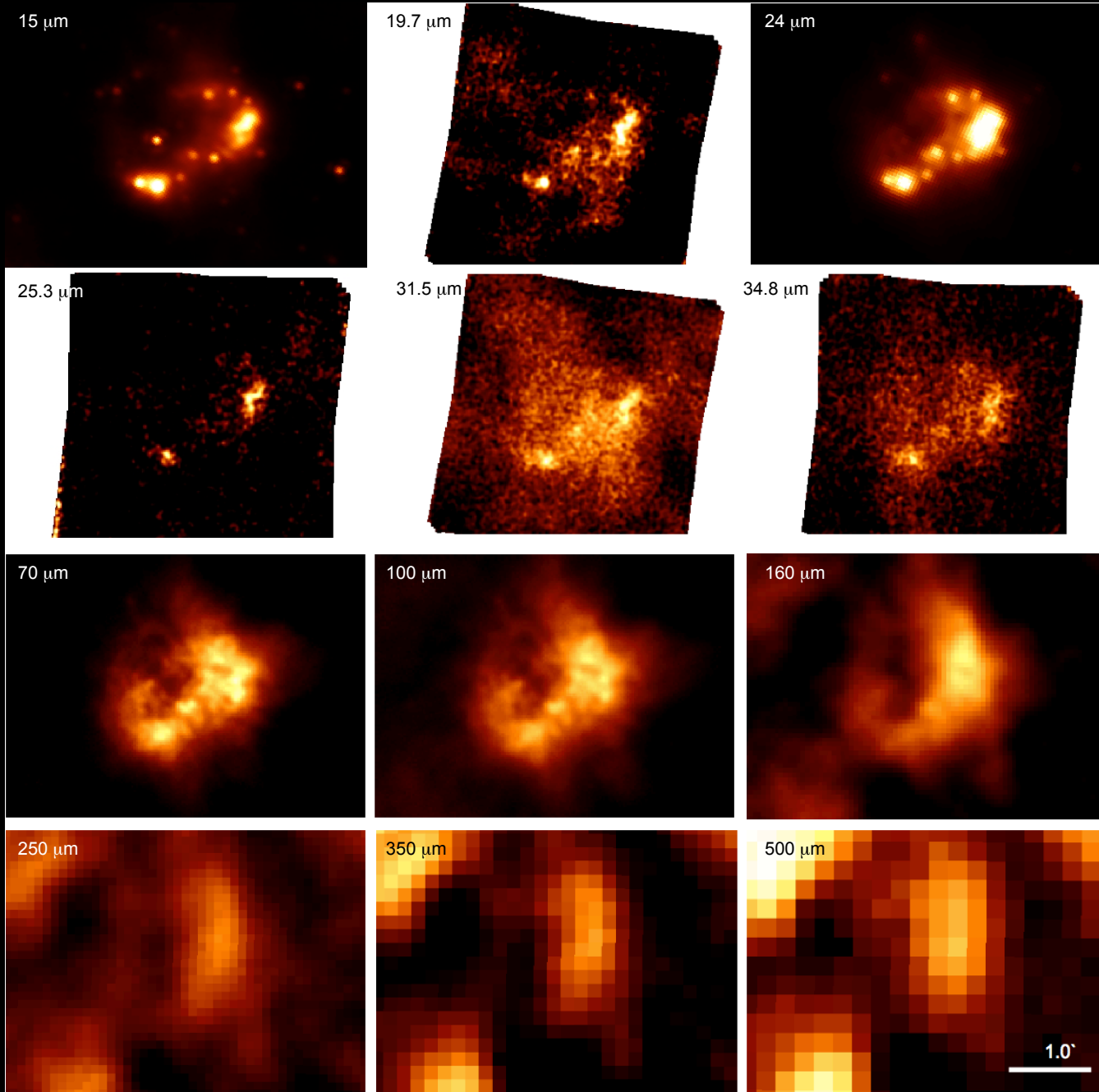


$V_{ej} = 500 \text{ km/s}$  at  $R_{PWN}$  consistent with  
 $M_{ej} = 10\text{-}15 M_{\odot}$  and  $E_{51} \sim 0.1 - 0.2$

# Follow-up Observations

- SOFIA – spatial resolution crucial for testing the radiatively-heated ejecta dust scenario
- *Herschel* – 70-500  $\mu\text{m}$  wavelength coverage to detect colder dust and characterize the dust mass

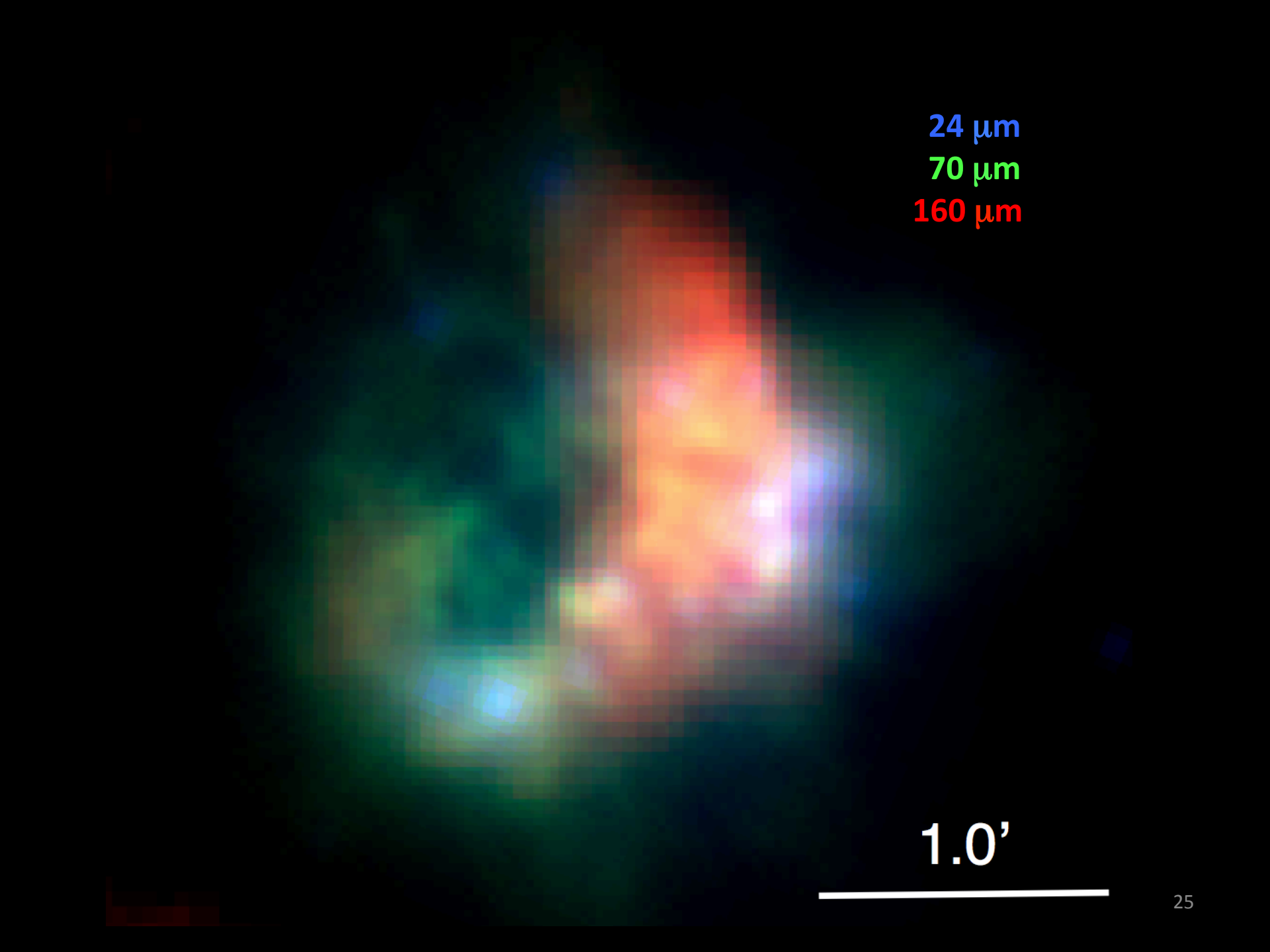
# SOFIA & Herschel (+ AKARI & Spitzer):



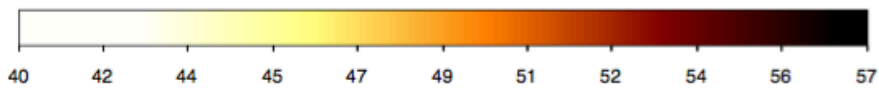
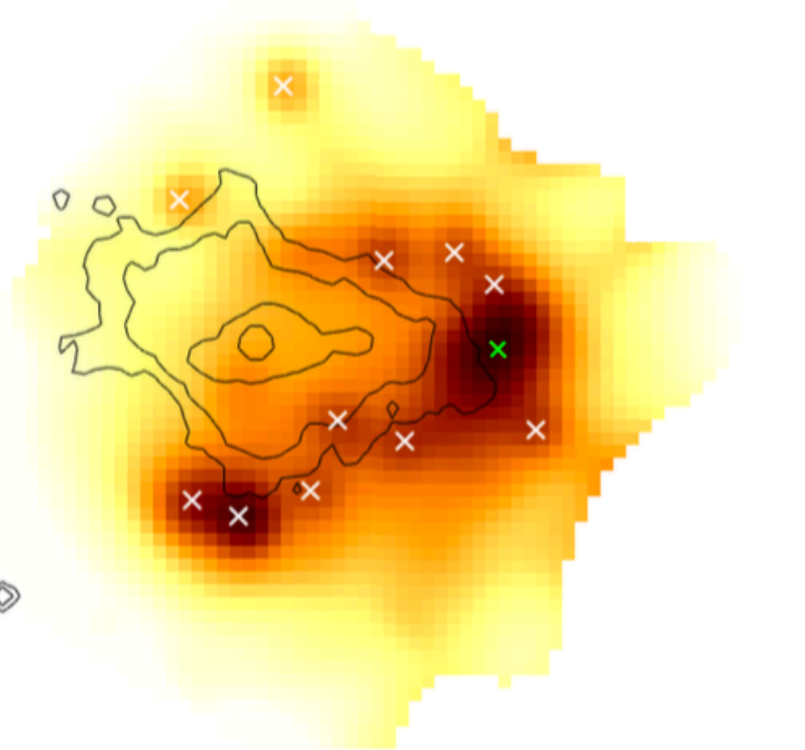


24  $\mu\text{m}$   
70  $\mu\text{m}$   
160  $\mu\text{m}$

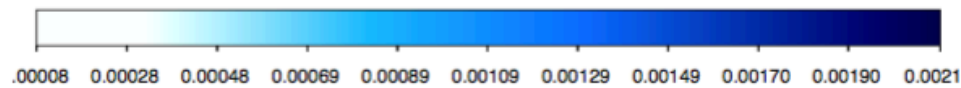
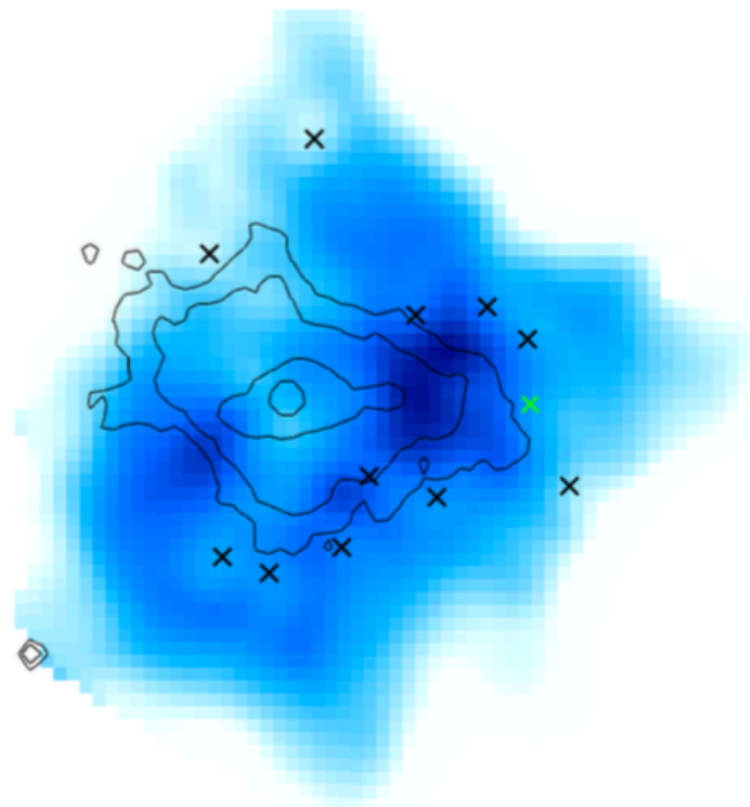
1.0'

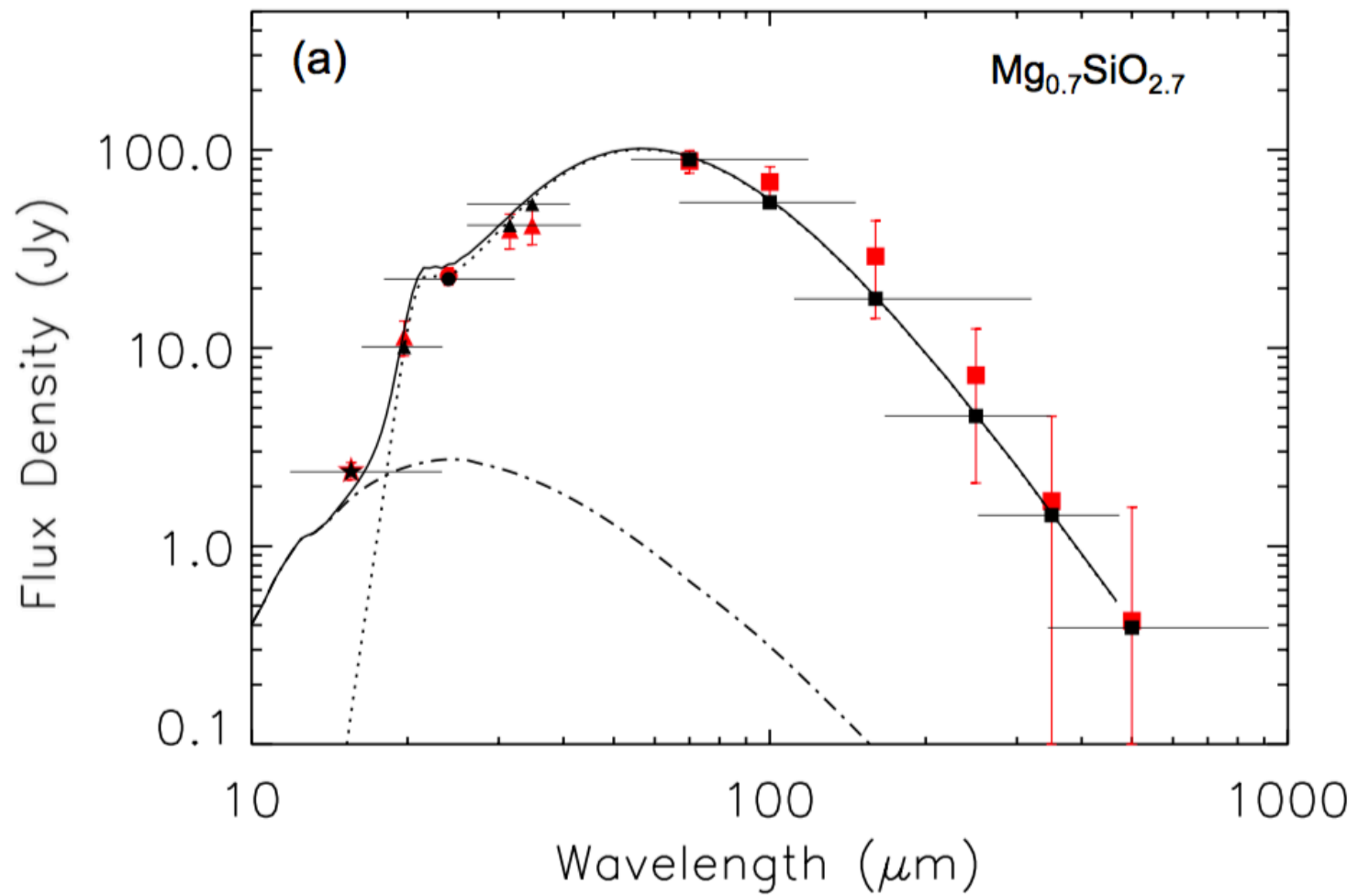
The image displays a multi-wavelength astronomical observation of a central source. The color gradient indicates different wavelengths: blue (shorter wavelength, 24 micrometers), green (intermediate wavelength, 70 micrometers), and red (longer wavelength, 160 micrometers). The central region is the brightest and most detailed, showing a complex structure with a color gradient from blue to red. The surrounding region is dimmer and more diffuse. A white scale bar is located at the bottom right, labeled '1.0''.

Temperature (K)

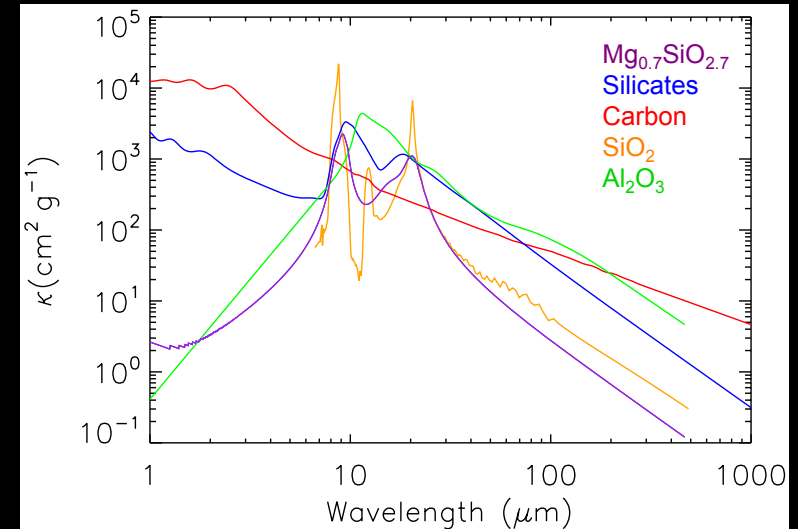
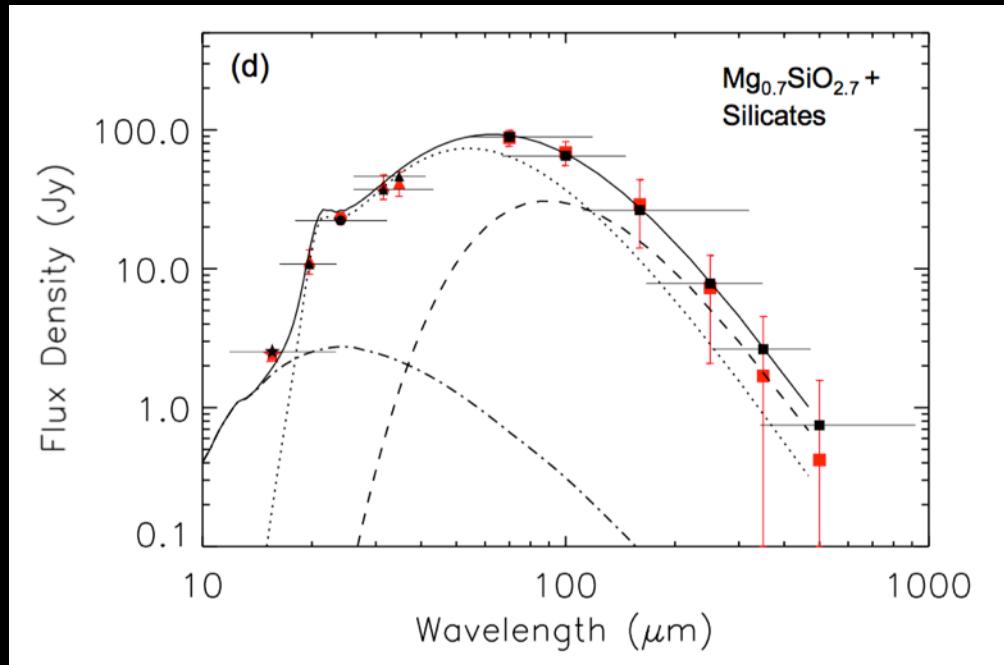


Dust Mass ( $M_{\odot}$ /pixel)





We estimated dust masses for a range of secondary component compositions:



At least  $0.3 M_{\odot}$  of SN dust!

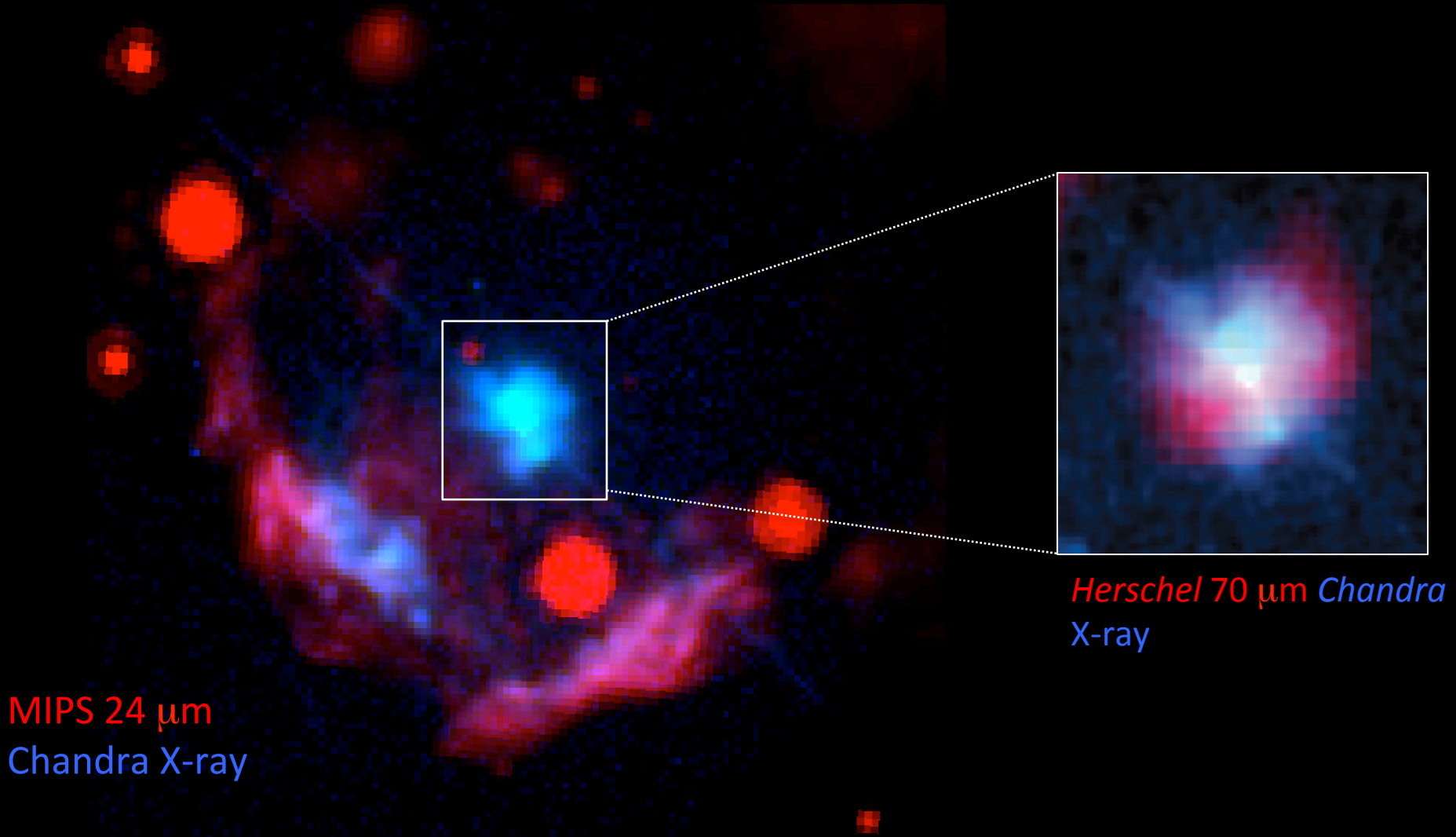
TABLE 3  
DUST MASSES ALLOWED BY NUCLEOSYNTHETIC YIELDS

$M_*$ ( $M_\odot$ )	$M_i$ ( $M_\odot$ )					$N_{\text{Mg}}/N_{\text{Si}}$	$M_d$ ( $M_\odot$ )			
	C	O	Mg	Al	Si		$\text{Mg}_{0.7}\text{SiO}_{2.7}$	$\text{MgO}+\text{SiO}_2$	$\text{Al}_2\text{O}_3$	$\text{Mg}_{0.7}\text{SiO}_{2.7} + \text{C}$
Woosley & Heger (2007):										
13.0	0.0949	0.5712	0.0505	0.0041	0.0707	0.83	0.222	0.234	0.008	0.316
14.0	0.1154	0.7229	0.0579	0.0046	0.0713	0.94	0.223	0.248	0.009	0.339
15.0	0.1336	0.8380	0.0525	0.0041	0.0742	0.82	0.232	0.245	0.008	0.366
16.0	0.1577	0.9371	0.0529	0.0041	0.0490	1.25	0.154	0.192	0.008	0.311
17.0	0.1768	1.3604	0.0826	0.0064	0.1715	0.56	0.427	0.502	0.012	0.604
18.0	0.1960	1.6358	0.1496	0.0137	0.1110	1.56	0.348	0.483	0.026	0.544
19.0	0.2077	1.8711	0.0985	0.0093	0.1358	0.84	0.426	0.452	0.018	0.633
20.0	0.2336	1.9604	0.1112	0.0089	0.2178	0.59	0.575	0.648	0.017	0.809
21.0	0.2701	2.5558	0.1536	0.0146	0.1296	1.37	0.406	0.530	0.028	0.676
22.0	0.2591	2.5249	0.1204	0.0117	0.2170	0.64	0.623	0.662	0.022	0.882
23.0	0.2986	2.5480	0.1478	0.0119	0.2556	0.67	0.764	0.789	0.022	1.063
24.0	0.2825	3.0035	0.2442	0.0207	0.2663	1.06	0.834	0.971	0.039	1.117
25.0	0.3629	3.3841	0.2307	0.0204	0.2990	0.89	0.937	1.018	0.039	1.300
26.0	0.3331	3.7727	0.1335	0.0154	0.3686	0.42	0.691	1.007	0.029	1.024
27.0	0.3159	4.0532	0.1674	0.0198	0.2937	0.66	0.866	0.903	0.037	1.182
28.0	0.3793	4.1549	0.2012	0.0229	0.1631	1.43	0.511	0.680	0.043	0.890
29.0	0.3828	4.8632	0.2474	0.0285	0.1788	1.60	0.560	0.789	0.054	0.943
30.0	0.4324	5.1512	0.3411	0.0328	0.1671	2.36	0.524	0.918	0.062	0.956
40.0	0.4501	6.4855	0.3656	0.0396	0.1627	2.60	0.510	0.949	0.075	0.960
60.0	6.1495	6.5599	0.1673	0.0168	0.2096	0.92	0.657	0.723	0.032	6.806
Sukhbold et al. (2016):										
12.7	0.1101	0.3886	0.0341	0.0022	0.0481	0.81	0.151	0.159	0.004	0.261
13.4	0.1177	0.5650	0.0489	0.0039	0.0551	1.03	0.172	0.198	0.007	0.290
13.8	0.1265	0.6189	0.0504	0.0038	0.0600	0.97	0.188	0.211	0.007	0.314
14.3	0.1365	0.7046	0.0563	0.0044	0.0606	1.08	0.190	0.222	0.008	0.326
14.7	0.1493	0.7608	0.0539	0.0041	0.0615	1.01	0.192	0.220	0.008	0.342
15.4	0.1718	0.9740	0.0628	0.0047	0.0825	0.89	0.259	0.279	0.009	0.430
16.2	0.1908	1.1489	0.0705	0.0052	0.0994	0.81	0.312	0.328	0.010	0.503
16.6	0.1973	1.2113	0.0748	0.0054	0.1047	0.82	0.329	0.347	0.010	0.526
17.0	0.2054	1.2862	0.0785	0.0056	0.1102	0.82	0.346	0.364	0.011	0.551
17.5	0.1974	1.5079	0.1216	0.0083	0.0790	1.78	0.247	0.368	0.016	0.445
18.1	0.1959	1.6296	0.1493	0.0136	0.1044	1.67	0.326	0.469	0.026	0.522
19.0	0.2133	1.9239	0.1239	0.0108	0.1426	1.59	0.277	0.508	0.020	0.490
20.1	0.2426	2.1250	0.0956	0.0101	0.3170	0.37	0.495	0.835	0.019	0.737
20.7	0.2278	2.4074	0.1343	0.0132	0.2163	1.53	0.396	0.683	0.025	0.624
21.4	0.2670	2.4646	0.1322	0.0120	0.0954	1.75	0.299	0.420	0.023	0.566
25.4	0.3765	3.5207	0.1051	0.0119	0.4236	0.28	0.540	1.078	0.022	0.917
25.9	0.3518	3.7937	0.1491	0.0179	0.4278	0.40	0.771	1.159	0.034	1.122
26.3	0.4097	3.7250	0.1423	0.0157	0.2861	0.57	0.730	0.845	0.030	1.140
27.2	0.4449	4.0087	0.1661	0.0188	0.2071	0.92	0.650	0.714	0.035	1.095
60.0	0.7750	3.4600	0.1234	0.0131	0.1071	1.31	0.336	0.430	0.025	1.111

Dust mass and composition indicate a 16-27  $M_\odot$  progenitor  
(consistent with Kim et al. 2013 & Gelfand et al. 2015)

# Kes 75: A dusty shell?

Pulsar age  $\sim 800$  yr, among youngest in the Galaxy (Gotthelf et al. 2000)

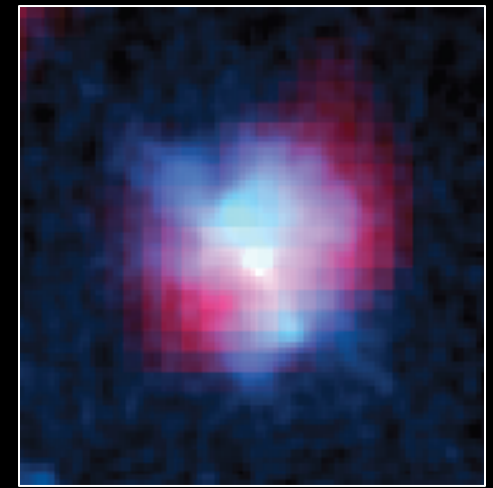


MIPS 24  $\mu\text{m}$   
Chandra X-ray

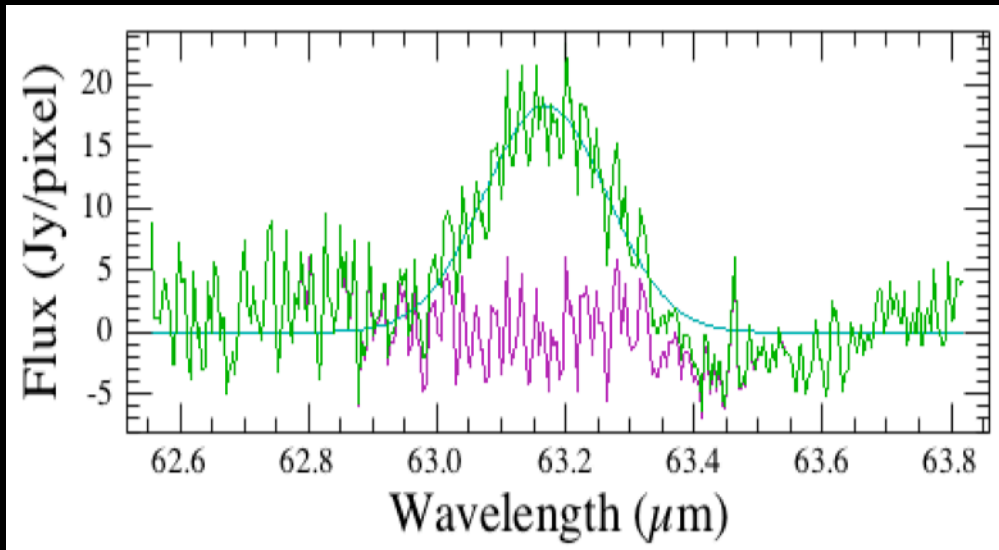
Herschel 70  $\mu\text{m}$  Chandra  
X-ray

# Kes 75: Herschel Spectroscopy

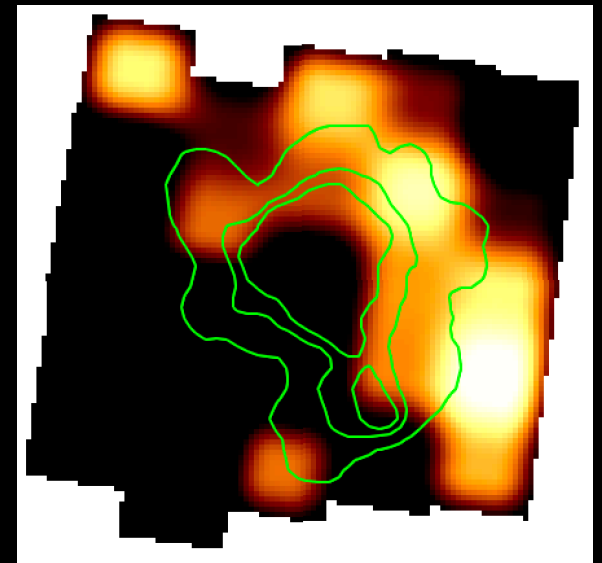
Ejecta velocity of  $\sim 500$  km/s



*Chandra*, *Herschel* 70  $\mu\text{m}$

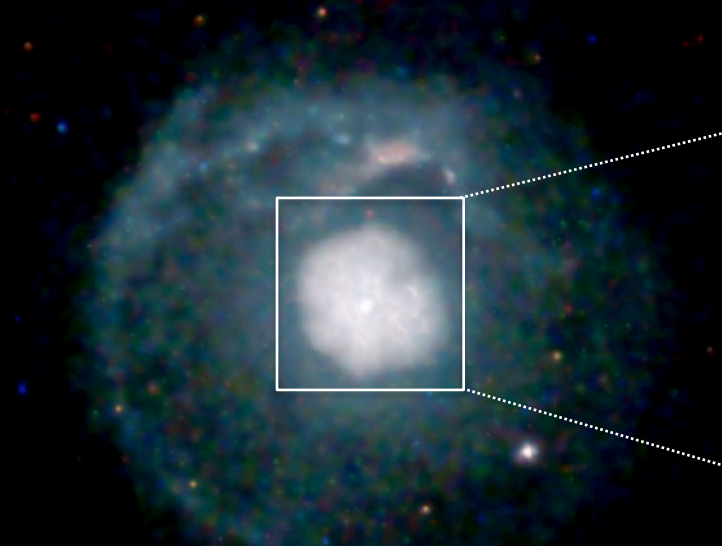


[O I] 63.18  $\mu\text{m}$  line, FWHM = 1000 km/s

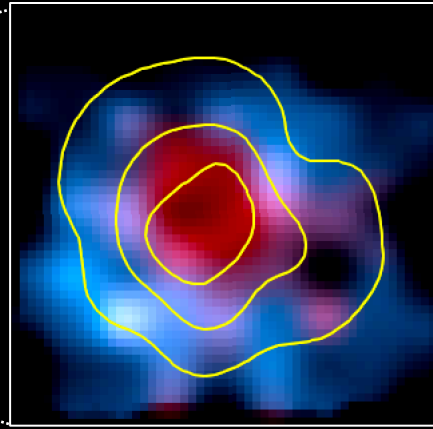


[O I] 63.18  $\mu\text{m}$  line image

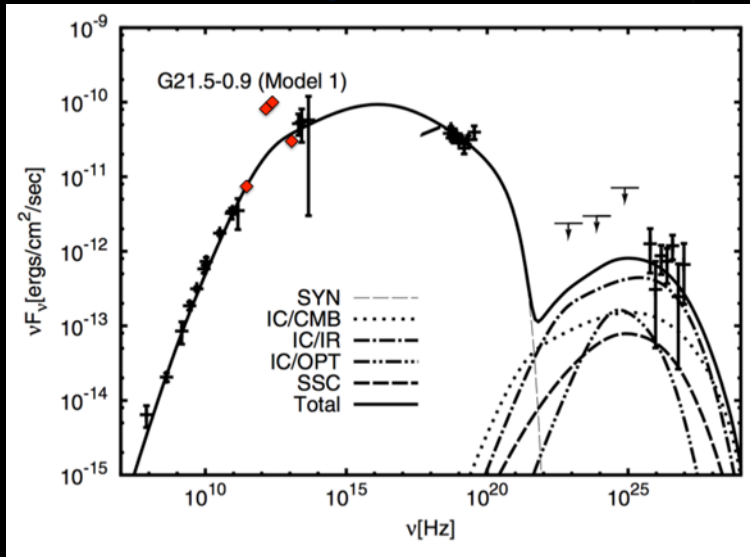
# G21.5-0.9: A shell of ejecta and dust



Chandra X-ray

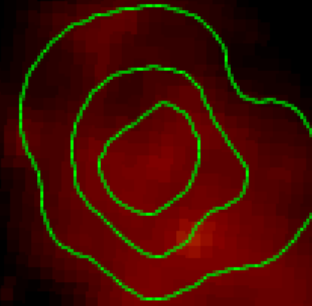


Herschel  
[C II] 157  $\mu\text{m}$  line  
ejecta velocity= 400 km/s



Tanaka & Takahara 2011

Far-IR excess 24 – 500  $\mu\text{m}$   $\rightarrow$  PWN-heated dust?



Spitzer 24  $\mu\text{m}$



# Summary

Emission from SN material around pulsar wind nebulae provides information on PWN/SNR dynamics, the ejecta properties, the progenitor star, and the properties of SN-formed dust.

Future modeling and searches for PWN-heated dust will help characterize composition, mass, and size distribution of pristine SN dust → give insight into the survival of grains and the contribution of core-collapse SNe to the dust budget in galaxies.